

SMU-HEP 94-25

ITP-SB-94-59

INLO-PUB-16/94

## Rates for Inclusive Deep-Inelastic Electroproduction of Charm Quarks at HERA

S. RIEMERSMA

*Department of Physics,  
Fondren Science Building,  
Southern Methodist University,  
Dallas, Texas 75275*

J. SMITH

*Institute for Theoretical Physics,  
State University of New York at Stony Brook,  
Stony Brook, New York 11794-3840*

and

W. L. VAN NEERVEN

*Instituut Lorentz,  
University of Leiden,  
P.O.B. 9506, 2300 RA, Leiden,  
The Netherlands.*

November 1994

### Abstract

The coefficient functions for heavy-flavour production in deeply inelastic electron-hadron scattering have been calculated previously. Analytic expressions are impossible to publish due to their length. Therefore we have tabulated them as two-dimensional arrays as is often done for the scale-dependent parton densities. Using this computer program we present event rates for charm production at HERA in bins of  $x$  and  $Q^2$ . These rates are insensitive to variations in the factorization and renormalization scale  $\mu$ .

In the past few years, calculations of  $O(\alpha_s)$  QCD corrections to heavy-flavour production have made great progress (for a recent review see [1]). Calculations have been completed for hadron-hadron collisions [2],[3], photoproduction [4],[5], electroproduction [6], [7], and photon-photon collisions (real as well as virtual photons) [8], [9]. The calculation of higher order corrections to these processes are important for the the top quark search [10] and the determination of the gluon distribution function [11], [12] which can be measured in open charm production.

The expressions are only available in large computer programs for the radiative corrections as their complexity prohibits publishing them in an analytic form. This complexity is due to the non-zero mass  $m$  of the heavy quark. If  $m$  were zero the final formulae could be constructed and published as is shown e.g., for the  $O(\alpha_s^2)$  corrections to the coefficient functions in deeply inelastic lepton-hadron scattering [13] and the Drell-Yan process [14]. In some special cases the use of lengthy computer programs can be avoided by either making approximations [15] or by making algebraic fits to the exact coefficient functions of heavy-flavour production in hadron-hadron collisions [2] and in photon-hadron scattering [5]. Such fits are quite accurate and enabled the authors in [16] to present complete tables of cross sections for charm, bottom and top production in many hadron-hadron reactions.

These algebraic fits mentioned above could be made because the coefficient functions calculated for heavy-flavour production in hadron-hadron and photon-hadron collisions only depend on one scale independent variable. This is in contrast with the coefficient functions of deeply inelastic heavy-flavour production which depend on two scale independent variables as the photon is virtual. Moreover it turns out that in the latter process the coefficient functions show a much more complicated behaviour than in the former ones so that an algebraic fit as presented in [2] is very difficult to achieve. Therefore we have constructed a set of tables reproducing the coefficient functions for each partonic subprocess in deeply inelastic electroproduction of heavy flavours. These tables are presented in the form of a two dimensional array in a computer program, analogous to the way various groups [17], [18] present the scale dependent parton densities in hadrons, which also depend on two variables. The computer program is available.<sup>1</sup> Our two-dimensional tables are used to predict the  $O(\alpha_s)$  corrected rates for inclusive charm production

---

<sup>1</sup>Requests should be sent to smith@elsebeth.physics.sunysb.edu.

at HERA by adding integrations over bins in  $x$  and  $Q^2$ . It will be interesting to compare our results with the forthcoming data from the ZEUS and H1 collaborations. Notice that in deeply inelastic electroproduction we only have to contend with the parton densities in the proton. In a later paper we will address the complications associated with predicting rates for heavy-flavour photoproduction (small  $Q^2$ ) which also involve the parton densities in the photon.

We begin by listing several important formulae. Omitting charged-current interactions, heavy-flavour production in deeply inelastic electron-proton scattering proceeds via the reaction

$$e^-(l_1) + P(p) \rightarrow e^-(l_2) + Q(p_1)(\bar{Q}(p_2)) + X. \quad (1)$$

Here  $X$  stands for any hadronic final state allowed by quantum number conservation. We sum over these states so that the process is inclusive with respect to the outgoing hadrons. When the virtuality  $-q^2$  ( $q = l_1 - l_2$ ) of the exchanged photon is not too large ( $-q^2 \ll M_Z^2$ ) the reaction in (1) is dominated by the one-photon exchange mechanism and we can neglect any weak interaction effects. If we also integrate over the heavy (anti)quark  $Q$  ( $\bar{Q}$ ) in the final state the deeply inelastic electroproduction cross section can be written as

$$\frac{d^2\sigma}{dx dy} = \frac{2\pi\alpha^2}{Q^4} S[\{1 + (1 - y)^2\}F_2(x, Q^2, m^2) - y^2 F_L(x, Q^2, m^2)], \quad (2)$$

where  $S$  denotes the square of the c.m. energy of the electron-proton system. The variables  $x$  and  $y$  are defined as

$$x = \frac{Q^2}{2p \cdot q} \quad (0 < x \leq 1) \quad , \quad y = \frac{p \cdot q}{p \cdot l_1} \quad (0 < y < 1), \quad (3)$$

with

$$-q^2 = Q^2 = xyS. \quad (4)$$

The deeply inelastic heavy-flavour structure functions appearing in the cross section (2) are given by  $F_2(x, Q^2, m^2)$  and  $F_L(x, Q^2, m^2)$  (longitudinal). The structure functions are given by the formula (see (6.5) of [6])

$$F_k(x, Q^2, m^2) = \frac{Q^2\alpha_s}{4\pi^2 m^2} \int_x^{z_{\max}} \frac{dz}{z} \left[ e_H^2 f_g\left(\frac{x}{z}, \mu^2\right) c_{k,g}^{(0)} \right]$$

$$\begin{aligned}
& + \frac{Q^2 \alpha_s^2}{\pi m^2} \int_x^{z_{\max}} \frac{dz}{z} \left[ e_H^2 f_g\left(\frac{x}{z}, \mu^2\right) (c_{k,g}^{(1)} + \bar{c}_{k,g}^{(1)} \ln \frac{\mu^2}{m^2}) \right. \\
& + \sum_{i=q, \bar{q}} \left[ e_H^2 f_i\left(\frac{x}{z}, \mu^2\right) (c_{k,i}^{(1)} + \bar{c}_{k,i}^{(1)} \ln \frac{\mu^2}{m^2}) \right. \\
& \left. \left. + e_{L,i}^2 f_i\left(\frac{x}{z}, \mu^2\right) (d_{k,i}^{(1)} + \bar{d}_{k,i}^{(1)} \ln \frac{\mu^2}{m^2}) \right] \right], \tag{5}
\end{aligned}$$

where  $k = 2, L$  and the upper boundary on the integration is given by  $z_{\max} = Q^2/(Q^2 + 4m^2)$ . Further  $f_i(x, \mu^2)$ , ( $i = g, q, \bar{q}$ ) denote the parton densities in the proton and  $\mu$  stands for the mass factorization scale, which has been put equal to the renormalization scale. The coefficient functions, represented by  $c_{k,i}^{(l)}(\eta, \xi)$ ,  $\bar{c}_{k,i}^{(l)}(\eta, \xi)$ , ( $i = g, q, \bar{q}; l = 0, 1$ ) and by  $d_{k,i}^{(l)}(\eta, \xi)$ ,  $\bar{d}_{k,i}^{(l)}(\eta, \xi)$ , ( $i = q, \bar{q}; l = 0, 1$ ) are calculated in [6] and they are represented in the  $\overline{\text{MS}}$  scheme. Furthermore they depend on the scaling variables  $\eta$  and  $\xi$  defined by

$$\eta = \frac{s}{4m^2} - 1 \quad , \quad \xi = \frac{Q^2}{m^2}. \tag{6}$$

where  $s$  is the square of the c.m. energy of the virtual photon-parton subprocess which implies that in (5)  $z = Q^2/(Q^2 + s)$ . In this equation we made a distinction between the coefficient functions with respect to their origin. The coefficient functions indicated by  $c_{k,i}^{(l)}(\eta, \xi)$ ,  $\bar{c}_{k,i}^{(l)}(\eta, \xi)$  originate from the partonic subprocesses where the virtual photon is coupled to the heavy quark whereas the quantities  $d_{k,i}^{(l)}(\eta, \xi)$ ,  $\bar{d}_{k,i}^{(l)}(\eta, \xi)$  come from the subprocess where the virtual photon interacts with the light quark. Hence the former are multiplied by the charge squared of the heavy quark  $e_H^2$ , whereas the latter are multiplied by the charge squared of the light quark  $e_L^2$  respectively (both in units of  $e$ ). Although terms proportional to  $e_H e_L$  appear in the inclusive photon-parton differential distributions they integrate to zero in the total partonic cross section, so we have not included them in (6). Furthermore we have isolated the factorization scale dependent term  $\ln(\mu^2/m^2)$ . The functions multiplied by this term, which are indicated by a bar, are called mass factorization parts. Notice that in the subsequent equations we discuss the transverse coefficient functions indicated by the subscript  $T$  instead of the ones indicated by the subscript 2. The relation between them is given by  $c_{2,i}^{(l)}(\eta, \xi) = c_{T,i}^{(l)}(\eta, \xi) + c_{L,i}^{(l)}(\eta, \xi)$  and  $d_{2,i}^{(l)}(\eta, \xi) = d_{T,i}^{(l)}(\eta, \xi) + d_{L,i}^{(l)}(\eta, \xi)$ . where the same definition holds for the coefficient functions indicated by a bar. In the limit  $\xi \rightarrow 0$  (see (6)) where the virtual photon becomes on-shell the

above coefficient functions tend to their analogues obtained for photoproduction which can be found in [4],[5]. For that purpose we had to modify the original expressions for the functions  $d_{k,q}^{(1)}(\eta, \xi)$ . Originally  $\bar{d}_{k,q}^{(1)}(\eta, \xi)$  did not exist because no mass factorization was needed and in the limit  $\xi \rightarrow 0$   $d_{T,q}^{(1)}(\eta, \xi)$  diverged logarithmically. This is due to an additional collinear divergence which appears when the virtual photon coupled to the light quark goes on-mass-shell. Furthermore in the same limit  $d_{L,q}^{(1)}(\eta, \xi)$  did not vanish. Therefore, to use these functions in the region  $\xi \approx 0$  one has to perform an additional mass factorization to remove the collinear divergence which is due to the on-shell photon. This is achieved by subtracting a term which is multiplied by a scale invariant function called  $R(\xi) = \exp(-20\xi)$  ( see (5.10) in [6] ) where the subtraction is imposed if  $Q^2 < Q_{min}^2 = 1.5 \text{ GeV}^2$ . This leads to the appearance of the function  $\bar{d}_{T,q}^{(1)}$  (  $\bar{d}_{L,q}^{(1)} = 0$  ) which would not have been present when the photon is treated to be highly virtual. This implies that the function  $\bar{d}_{T,q}^{(1)}$  will be proportional to  $R(\xi)$  and it vanishes when  $\xi \rightarrow \infty$ . Notice that our choice of  $R$  in [6] was not scale independent so that the plot 11.b in that paper still contains a scale dependence. This however has no consequence for any of the numerical results. The above procedure implies that in the on-mass-shell limit the function  $d_{L,q}^{(1)}(\eta, 0) = 0$  and  $d_{T,q}^{(1)}(\eta, 0), \bar{d}_{T,q}^{(1)}(\eta, 0)$  become equal to the on-mass-shell photon coefficient functions in [4], [5] (see (2.11) and (2.15) in [4]).

The coefficient functions for the Born reaction (virtual photon-gluon fusion, see [19]) are given by

$$c_{L,g}^{(0)}(\eta, \xi) = \frac{\pi T_f}{2} \frac{\xi}{(1 + \eta + \xi/4)^3} \left[ 2(\eta(1 + \eta))^{1/2} - \ln \frac{(1 + \eta)^{1/2} + \eta^{1/2}}{(1 + \eta)^{1/2} - \eta^{1/2}} \right], \quad (7)$$

$$c_{T,g}^{(0)}(\eta, \xi) = \frac{\pi T_f}{2} \frac{1}{(1 + \eta + \xi/4)^3} \left[ -2 \left\{ (1 + \eta - \xi/4)^2 + 1 + \eta \right\} \left( \frac{\eta}{1 + \eta} \right)^{1/2} + \left\{ 2(1 + \eta)^2 + \frac{\xi^2}{8} + 1 + 2\eta \right\} \ln \frac{(1 + \eta)^{1/2} + \eta^{1/2}}{(1 + \eta)^{1/2} - \eta^{1/2}} \right], \quad (8)$$

where  $T_f = 1/2$  in  $SU(N)$ .

No such simple analytic expressions can be given for the next to leading order coefficient functions. Therefore we present them in tables constructed

as follows. First we ran the programs in [6] and computed the coefficient functions for a grid of values of  $\eta$  and  $\xi$  as defined in (6). This we have only done when they are represented in the  $\overline{\text{MS}}$  scheme. We then divided these functions by the appropriate colour factor and then subtracted the asymptotic and threshold dependences, for which analytic expressions are available in the literature and will be presented below. Finally we wrote subroutines to set up two dimensional arrays. The interpolation is done in a bilinear fashion [21].

Starting with the virtual-gluon subprocess we define a new function with the threshold and asymptotic behavior removed, namely

$$h_{A,k,g}^{(1)}(\eta, \xi) = (C_A T_f)^{-1} c_{A,k,g}^{(1)}(\eta, \xi) - \beta G_k(\eta, \xi) - \rho E_{k,A}(\eta, \xi), \quad (9)$$

and

$$h_{F,k,g}^{(1)}(\eta, \xi) = (C_A T_f)^{-1} c_{F,k,g}^{(1)}(\eta, \xi) - \rho E_{k,F}(\eta, \xi). \quad (10)$$

Here we have split the coefficient functions  $c_{k,g}^{(1)}$  according to their colour parts indicated by the subscripts  $A$  and  $F$ . The colour factors are given by  $C_A T_f$  and  $C_F T_f$  respectively, where for  $SU(N)$ ,  $C_A = N$  and  $C_F = (N^2 - 1)/2N$ . Further we have defined

$$\beta = \left( \frac{\eta}{1 + \eta} \right)^{1/2}, \quad \rho = \frac{1}{1 + \eta}. \quad (11)$$

The mass factorization parts  $\bar{c}_{k,g}(\eta, \xi)$  can be parameterized in a similar way by

$$\bar{h}_{k,g}^{(1)}(\eta, \xi) = (C_A T_f)^{-1} \bar{c}_{k,g}^{(1)}(\eta, \xi) - \beta \bar{G}_k(\eta, \xi) - \rho \bar{E}_{k,A}(\eta, \xi). \quad (12)$$

The functions  $E_{k,C}, \bar{E}_{k,C}$  with  $k = T, L$  and  $C = A, F$  describe the threshold behaviour as  $\eta \rightarrow 0$  (or as  $s \rightarrow 4m^2$ ) and are derived from (5.7)-(5.9) of [6]<sup>2</sup>. The asymptotic behavior which holds in the region  $\eta \rightarrow \infty$  (or as  $(s \rightarrow \infty)$ ) is given by the functions  $G_k, \bar{G}_k$  with  $k = T, L$ . The latter are obtained from [20] (see their Appendix A). The functions describing the threshold region have the following form

$$E_{L,F}(\eta, \xi) = \frac{1}{6\pi} \frac{\xi}{(1 + \xi/4)^3} \beta^2 \left[ \frac{\pi^2}{2} \right], \quad (13)$$

---

<sup>2</sup>Notice that an extra factor of two should be multiplied to (5.9) of [6]

$$E_{T,F}(\eta, \xi) = \frac{1}{4\pi} \frac{1}{1 + \xi/4} \left[ \frac{\pi^2}{2} \right], \quad (14)$$

$$E_{L,A}(\eta, \xi) = \frac{1}{6\pi} \frac{\xi}{(1 + \xi/4)^3} \beta^2 \left[ \beta \ln^2(8\beta^2) - 5\beta \ln(8\beta^2) - \frac{\pi^2}{4} \right], \quad (15)$$

$$E_{T,A}(\eta, \xi) = \frac{1}{4\pi} \frac{1}{(1 + \xi/4)} \left[ \beta \ln^2(8\beta^2) - 5\beta \ln(8\beta^2) - \frac{\pi^2}{4} \right], \quad (16)$$

$$\bar{E}_{L,A}(\eta, \xi) = \frac{1}{6\pi} \frac{\xi}{(1 + \xi/4)^3} \beta^3 \left[ -\ln(4\beta^2) \right], \quad (17)$$

$$\bar{E}_{T,A}(\eta, \xi) = \frac{1}{4\pi} \frac{1}{1 + \xi/4} \beta \left[ -\ln(4\beta^2) \right]. \quad (18)$$

The functions describing the asymptotic region are given by

$$G_L(\eta, \xi) = \frac{1}{6\pi} \left[ \frac{4}{\xi} - \frac{4}{3} \frac{1}{1 + \xi/4} + \left( 1 - \frac{2}{\xi} - \frac{1}{6} \frac{1}{1 + \xi/4} \right) J(\xi) - \left( \frac{3}{\xi} + \frac{1}{4} \frac{1}{1 + \xi/4} \right) I(\xi) \right], \quad (19)$$

$$G_T(\eta, \xi) = \frac{1}{6\pi} \left[ -\frac{21}{3\xi} + \frac{4}{3} \frac{1}{1 + \xi/4} + \left( \frac{7}{6} + \frac{11}{3\xi} + \frac{1}{6} \frac{1}{1 + \xi/4} \right) J(\xi) + \left( 1 + \frac{2}{\xi} + \frac{1}{4} \frac{1}{1 + \xi/4} \right) I(\xi) \right], \quad (20)$$

$$\bar{G}_L(\eta, \xi) = \frac{1}{6\pi} \left[ -\frac{6}{\xi} + \frac{1}{2} \frac{1}{1 + \xi/4} + \left( \frac{3}{\xi} + \frac{1}{4} \frac{1}{1 + \xi/4} \right) J(\xi) \right], \quad (21)$$

$$\bar{G}_T(\eta, \xi) = \frac{1}{6\pi} \left[ \frac{4}{\xi} - \frac{1}{2} \frac{1}{1 + \xi/4} - \left( 1 + \frac{2}{\xi} + \frac{1}{4} \frac{1}{1 + \xi/4} \right) J(\xi) \right], \quad (22)$$

where the functions  $J(\xi)$  and  $I(\xi)$  are defined by (see Appendix A in [20])

$$J(\xi) = \frac{4}{(\xi(4 + \xi))^{1/2}} \ln \left( \frac{(4 + \xi)^{1/2} + \xi^{1/2}}{(4 + \xi)^{1/2} - \xi^{1/2}} \right), \quad (23)$$

$$I(\xi) = \frac{4}{(\xi(4+\xi))^{1/2}} \left[ -\frac{\pi^2}{6} - \frac{1}{2} \ln^2 \left( \frac{(4+\xi)^{1/2} + \xi^{1/2}}{(4+\xi)^{1/2} - \xi^{1/2}} \right) + \ln^2 \left( \frac{(4+\xi)^{1/2} - \xi^{1/2}}{2(4+\xi)^{1/2}} \right) + 2\text{Li}_2 \left( \frac{(4+\xi)^{1/2} - \xi^{1/2}}{2(4+\xi)^{1/2}} \right) \right], \quad (24)$$

where  $\text{Li}_2(x)$  is the dilogarithmic function defined as

$$\text{Li}_2(x) = -\int_0^x \frac{dt}{t} \ln(1-t). \quad (25)$$

We proceed in an analogous way for the coefficient functions corresponding to the virtual photon-light quark subprocesses. When the photon is coupled to the heavy flavour they are parameterized as

$$h_{H,k,q}^{(1)}(\eta, \xi) = (C_F T_f)^{-1} c_{k,q}^{(1)}(\eta, \xi) - \beta^3 G_k(\eta, \xi), \quad (26)$$

and

$$\bar{h}_{H,k,q}^{(1)}(\eta, \xi) = (C_F T_f)^{-1} \bar{c}_{k,q}^{(1)}(\eta, \xi) - \beta^3 \bar{G}_k(\eta, \xi). \quad (27)$$

When the photon is coupled to the light quark we get

$$h_{L,k,q}^{(1)}(\eta, \xi) = (C_F T_f)^{-1} d_{k,q}^{(1)}(\eta, \xi), \quad (28)$$

and

$$\bar{h}_{L,k,q}^{(1)}(\eta, \xi) = (C_F T_f)^{-1} \bar{d}_{k,q}^{(1)}(\eta, \xi). \quad (29)$$

The subscripts  $H$  and  $L$  in the above expressions indicate that when they are inserted in (5) they have to be multiplied by the charge factors  $e_H^2$  and  $e_L^2$  respectively.

Notice that for the reactions discussed above only the  $A$ -part of the coefficient functions show an enhancement in both the threshold region and the asymptotic region. For the  $F$ -part we only observe large corrections in the threshold region except for the process given by the expressions in (28) and (29). To illustrate the quality of the fits, we present the plots of the coefficient functions which constitute the bulk of the  $O(\alpha_s)$  radiative correction. They are given by  $h_{A,T,g}^{(1)}$  (9) and  $h_{F,T,g}^{(1)}$  (10), which are shown in fig.1 and fig.2 respectively. They are plotted versus  $\eta$  for several different values of  $\xi$ .

(One can compare them with the plots in [6] for the corresponding functions without the subtraction of the threshold and asymptotic behavior.) In both instances, we observe that the  $h$  functions tend to zero as  $\eta \rightarrow 0$  and as  $\eta \rightarrow \infty$ . Also, as  $\xi \rightarrow \infty$ , the  $h$  functions become zero across the entire  $\eta$ -region. We also see the complicated behaviour of the functions in the intermediate region which illustrates why an algebraic parameterization is very difficult to accomplish.

Using the fits, we now present single-particle inclusive event rates for inclusive  $c$  production given an integrated luminosity of  $300 \text{ nb}^{-1}$  at  $\sqrt{S} = 298 \text{ GeV}$ . Notice that we consider charm production only and do not sum over the charm and anti-charm cross sections. We take  $m_c = 1.6 \text{ GeV}/c^2$  and vary the mass factorization scale  $\mu = \sqrt{Q^2 + m^2}$  up and down by a factor of two. Furthermore we have chosen the CTEQ2M parton densities [17] and the two-loop running coupling constant with  $\Lambda_{\text{QCD}}^{(4)} = 213 \text{ MeV}$ . Our results are listed in tables 1 and 2 where we computed the cross section in (2) in bins of  $x$  and  $Q^2$  (these are the bins used by the ZEUS collaboration in their 1993 data for  $F_2$ ). Table 1 contains the event numbers for the lower  $Q^2$  bins and Table 2 the corresponding numbers for the higher  $Q^2$  bins.

We find the events concentrated at low  $Q^2$  and  $x$ , with an approximate five percent uncertainty at small  $x$  coming from the variation in the scale  $\mu$ . In the intermediate  $Q^2$  and  $x$  region, we find the number of events stable and significant. As  $Q^2$  increases, the number of events drops rapidly. However, here we expect weak interaction effects to reduce the applicability of the one-photon exchange approximation. To conclude, we see that the number of charm events is large and relatively insusceptible to variations in the scale. From these results and the good luminosity at HERA, the extraction of the gluon density with significantly reduced uncertainty should be possible.

### Acknowledgements

We thank J. Whitmore for useful discussions. S.Riemersma thanks the ITP at Stony Brook for their hospitality and the Lightner-Sams Foundation, Inc. for assistance in providing computing facilities. The research of J. Smith is supported in part by the contract NSF 9309888.

$Q^2$	$Q^2$	$x$	$x$	Events		
(GeV <sup>2</sup> )	range		range	$\mu = M/2$	$\mu = M$	$\mu = M$
8.5	7 - 10	$4.2 \cdot 10^{-4}$	$3.0 - 6.0 \cdot 10^{-4}$	228	205	204
		$8.5 \cdot 10^{-4}$	$6.0 - 12.0 \cdot 10^{-4}$	196	176	173
12	10 - 14	$4.2 \cdot 10^{-4}$	$3.0 - 6.0 \cdot 10^{-4}$	182	169	170
		$8.5 \cdot 10^{-4}$	$6.0 - 12.0 \cdot 10^{-4}$	164	152	151
		$1.6 \cdot 10^{-3}$	$1.2 - 2.0 \cdot 10^{-3}$	102	94	93
		$2.7 \cdot 10^{-3}$	$2.0 - 3.6 \cdot 10^{-3}$	95	88	86
15	14 - 20	$4.2 \cdot 10^{-4}$	$3.0 - 6.0 \cdot 10^{-4}$	153	143	144
		$8.5 \cdot 10^{-4}$	$6.0 - 12.0 \cdot 10^{-4}$	148	137	137
		$1.6 \cdot 10^{-3}$	$1.2 - 2.0 \cdot 10^{-3}$	94	88	86
		$2.7 \cdot 10^{-3}$	$2.0 - 3.6 \cdot 10^{-3}$	90	83	81
		$4.7 \cdot 10^{-3}$	$3.6 - 6.0 \cdot 10^{-3}$	62	57	55
25	20 - 28	$4.2 \cdot 10^{-4}$	$3.0 - 6.0 \cdot 10^{-4}$	104	99	100
		$8.5 \cdot 10^{-4}$	$6.0 - 12.0 \cdot 10^{-4}$	108	103	103
		$1.6 \cdot 10^{-3}$	$1.2 - 2.0 \cdot 10^{-3}$	72	69	68
		$2.7 \cdot 10^{-3}$	$2.0 - 3.6 \cdot 10^{-3}$	70	67	65
		$4.7 \cdot 10^{-3}$	$3.6 - 6.0 \cdot 10^{-3}$	49	46	45
35	28 - 40	$8.5 \cdot 10^{-4}$	$6.0 - 12.0 \cdot 10^{-4}$	87	86	87
		$1.6 \cdot 10^{-3}$	$1.2 - 2.0 \cdot 10^{-3}$	62	61	61
		$2.7 \cdot 10^{-3}$	$2.0 - 3.6 \cdot 10^{-3}$	62	61	61
		$4.7 \cdot 10^{-3}$	$3.6 - 6.0 \cdot 10^{-3}$	45	43	42
		$7.7 \cdot 10^{-3}$	$6.0 - 10.0 \cdot 10^{-3}$	35	34	33
50	40 - 56	$8.5 \cdot 10^{-4}$	$6.0 - 12.0 \cdot 10^{-4}$	58	59	61
		$1.6 \cdot 10^{-3}$	$1.2 - 2.0 \cdot 10^{-3}$	45	45	46
		$2.7 \cdot 10^{-3}$	$2.0 - 3.6 \cdot 10^{-3}$	47	47	47
		$4.7 \cdot 10^{-3}$	$3.6 - 6.0 \cdot 10^{-3}$	34	34	34
		$7.7 \cdot 10^{-3}$	$6.0 - 10.0 \cdot 10^{-3}$	27	27	27
		$1.4 \cdot 10^{-2}$	$1.0 - 2.0 \cdot 10^{-2}$	28	27	26
65	56 - 80	$1.6 \cdot 10^{-3}$	$1.2 - 2.0 \cdot 10^{-3}$	33	33	33
		$2.7 \cdot 10^{-3}$	$2.0 - 3.6 \cdot 10^{-3}$	37	36	36
		$4.7 \cdot 10^{-3}$	$3.6 - 6.0 \cdot 10^{-3}$	28	27	27
		$7.7 \cdot 10^{-3}$	$6.0 - 10.0 \cdot 10^{-3}$	23	22	22
		$1.4 \cdot 10^{-2}$	$1.0 - 2.0 \cdot 10^{-2}$	23	22	21

$Q^2$	$Q^2$	$x$	$x$	Events		
(GeV <sup>2</sup> )	range		range	$\mu = M/2$	$\mu = M$	$\mu = M$
125	80 - 160	$1.6 \cdot 10^{-3}$	$1.2 - 2.0 \cdot 10^{-3}$	28	28	28
		$2.7 \cdot 10^{-3}$	$2.0 - 3.6 \cdot 10^{-3}$	41	41	41
		$4.7 \cdot 10^{-3}$	$3.6 - 6.0 \cdot 10^{-3}$	33	33	33
		$7.7 \cdot 10^{-3}$	$6.0 - 10.0 \cdot 10^{-3}$	29	28	28
		$1.4 \cdot 10^{-2}$	$1.0 - 2.0 \cdot 10^{-2}$	29	29	28
		$2.8 \cdot 10^{-2}$	$2.0 - 4.0 \cdot 10^{-2}$	19	18	17
250	160 - 320	$4.7 \cdot 10^{-3}$	$3.6 - 6.0 \cdot 10^{-3}$	15	15	15
		$7.7 \cdot 10^{-3}$	$6.0 - 10.0 \cdot 10^{-3}$	15	14	14
		$1.4 \cdot 10^{-2}$	$1.0 - 2.0 \cdot 10^{-2}$	16	16	15
		$2.8 \cdot 10^{-2}$	$2.0 - 4.0 \cdot 10^{-2}$	11	10	10
		$5.7 \cdot 10^{-2}$	$4.0 - 8.0 \cdot 10^{-2}$	6.2	5.8	5.3
500	320 - 640	$7.7 \cdot 10^{-3}$	$6.0 - 10.0 \cdot 10^{-3}$	6.0	6.0	5.9
		$1.4 \cdot 10^{-2}$	$1.0 - 2.0 \cdot 10^{-2}$	7.6	7.5	7.3
		$2.8 \cdot 10^{-2}$	$2.0 - 4.0 \cdot 10^{-2}$	5.6	5.4	5.2
		$5.7 \cdot 10^{-2}$	$4.0 - 8.0 \cdot 10^{-2}$	3.3	3.2	2.9
		0.11	$8.0 - 16.0 \cdot 10^{-2}$	1.5	1.4	1.2
1000	640 - 1280	$1.4 \cdot 10^{-2}$	$1.0 - 2.0 \cdot 10^{-2}$	2.7	2.6	2.5
		$2.8 \cdot 10^{-2}$	$2.0 - 4.0 \cdot 10^{-2}$	2.5	2.4	2.2
		$5.7 \cdot 10^{-2}$	$4.0 - 8.0 \cdot 10^{-2}$	1.6	1.5	1.4
		0.11	$8.0 - 16.0 \cdot 10^{-2}$	0.75	0.67	0.59
2000	1280 - 2560	$2.8 \cdot 10^{-2}$	$2.0 - 4.0 \cdot 10^{-2}$	0.90	0.87	0.83
		$5.7 \cdot 10^{-2}$	$4.0 - 8.0 \cdot 10^{-2}$	0.72	0.69	0.64
		0.11	$8.0 - 16.0 \cdot 10^{-2}$	0.37	0.34	0.30
5000	2560 - 10000	0.11	$8.0 - 16.0 \cdot 10^{-2}$	0.17	0.13	0.096

## References

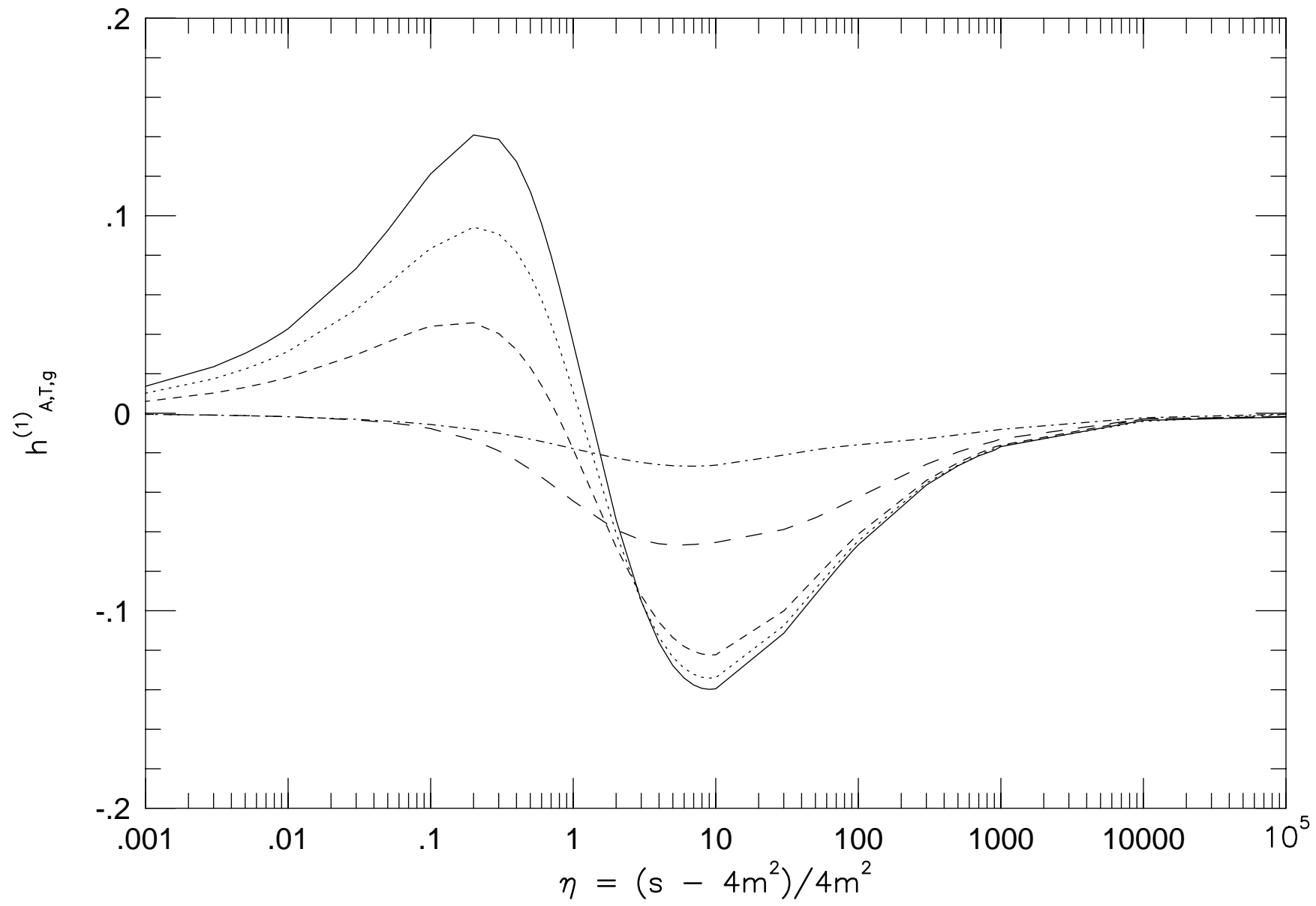
- [1] J. Smith and W.K Tung, in Proceedings of the Workshop on B Physics at Hadron Accelerators, Snowmass, Co. June, 1993 edited by P. McBride and S. Shekhar Mishra, Fermilab CONF-93/267, p19.
- [2] P. Nason, S. Dawson and R.K. Ellis, Nucl. Phys. B303 (1988) 607; B327 (1989) 49 (Erratum B335 (1990) 260).
- [3] W. Beenakker, H. Kuijf, W.L. van Neerven and J. Smith, Phys. Rev. D40 (1989) 54; W. Beenakker, W.L. van Neerven, R. Meng, G.A. Schuler and J. Smith, Nucl. Phys. B351 (1991) 507.
- [4] R.K. Ellis and P. Nason, Nucl. Phys. B312 (1989) 551.
- [5] J. Smith and W.L. van Neerven, Nucl. Phys. B374 (1992) 36.
- [6] E. Laenen, S. Riemersma, J. Smith and W.L. van Neerven, Nucl. Phys. B392 (1993) 162, 229; Phys. Lett. B291 (1992) 325.
- [7] M.A.G. Aivazis, F.I. Olness and W.-K. Tung, Phys. Rev. D50 (1994), 3085; M.A.G. Aivazis, J.C. Collins, F.I. Olness and W.-K. Tung, Phys. Rev. D50 (1994), 3102; F.I. Olness and S. Riemersma, SMU-HEP 94-21.
- [8] M. Drees, M Krämer, J. Zunft and P.M. Zerwas, Phys. Lett. B306 (1993) 371; J.H. Kühn, E. Mirkes and J. Steegborn, Z. Phys. C57 (1993) 615; O.J.P. Éboli, M.C. Gonzalez-Garcia, F. Halzen and S.F. Novaes, Phys. Rev. D47 (1993) 1889.
- [9] E. Laenen, S. Riemersma, J. Smith and W.L. van Neerven, Phys. Rev. D49 (1993) 5753.
- [10] (CDF collaboration) F. Abe et al., Phys. Rev. 50 (1994) 2966; (D0 Collaboration) S. Abachi, et al., Fermilab-PUB-345/E.
- [11] A. Ali and D. Wyler "Heavy Quark Physics at HERA: Introduction and Overview", in Physics at HERA, Proceedings of the Workshop, Hamburg, Oct. 29-30, 1991 Eds. W. Buchmüller and G. Ingelman, vol 2, p.669. R. van Woudenberg et al "Gluon density determination from open charm events at HERA", same proceedings Vol.2 p.739.

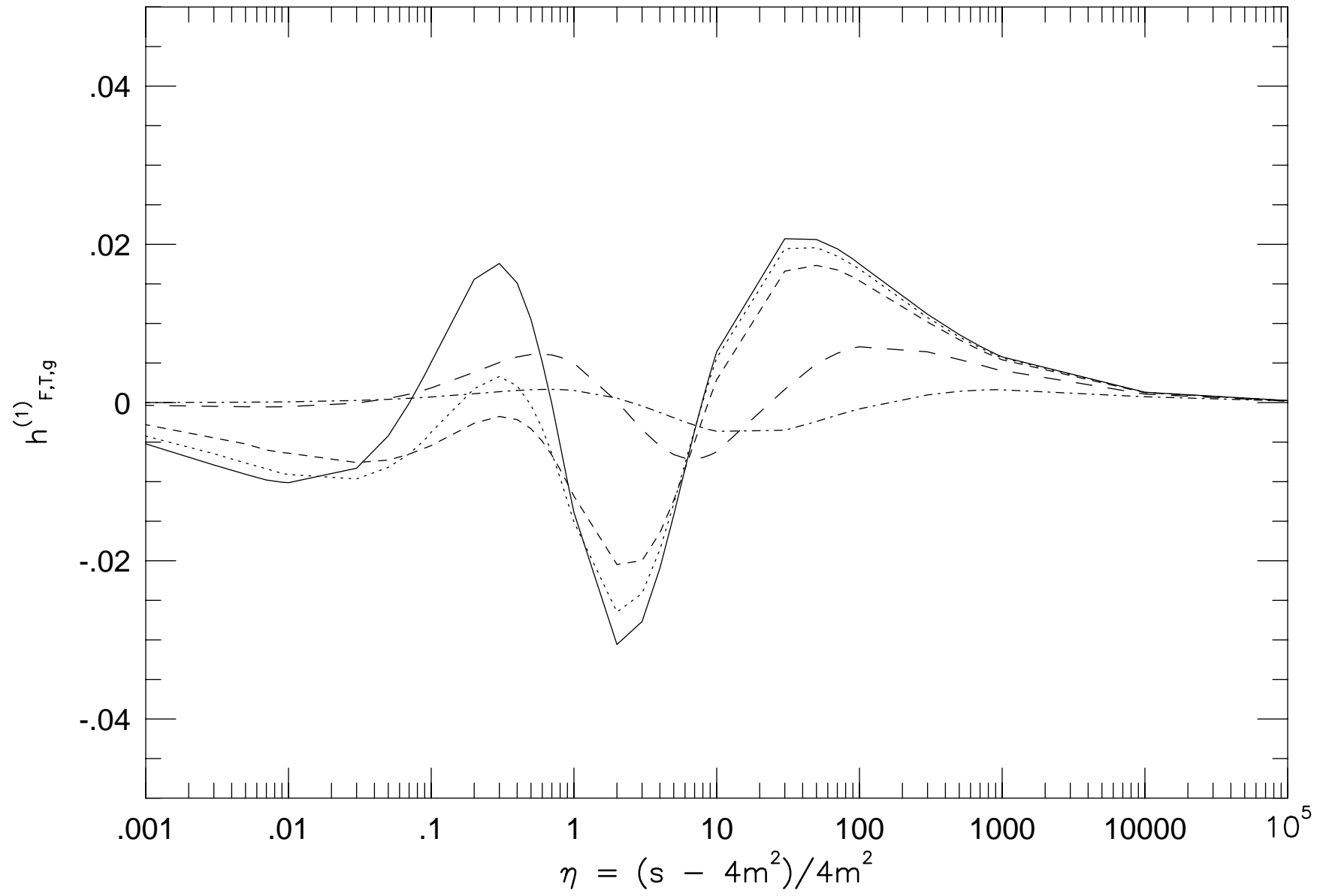
- [12] M. Glück, E. Reya and M. Stratmann, Nucl.Phys. B422 (1994) 37.
- [13] E.B. Zijlstra and W.L. van Neerven, Nucl. Phys. B383 (1992) 525; Phys. Lett. B273 (1991) 476; W.L. van Neerven and E.B. Zijlstra, Phys.Lett. B272 (1991) 127.
- [14] R. Hamberg, W.L. van Neerven and T. Matsuura, Nucl. Phys. B359 (1991) 343; W.L. van Neerven and E.B. Zijlstra, Nucl. Phys. B382 (1992) 11.
- [15] R. Meng, G.A. Schuler, J. Smith and W.L. van Neerven, Nucl. Phys. B339 (1990) 325.
- [16] G. Altarelli, M. Diemoz, G. Martinelli and P. Nason, Nucl. Phys. B308 (1988) 724.
- [17] J. Botts, H.L. Lai, J.G. Morfín, J.F. Owens, J.W. Qiu, W-K. Tung, and H. Weerts, Phys. Letts. B304 (1993) 159.
- [18] A.D. Martin, W.J. Stirling and R.G. Roberts, Phys. Rev. D47 (1993) 867; Phys. Letts. B306, (1993) 145; Erratum Phys. Letts B309 (1993) 492.
- [19] E. Witten, Nucl. Phys. B104 (1976) 445; J. Babcock and D. Sivers, Phys. Rev. D18 (1978) 2301; M.A. Shifman, A.I. Vainstein and V.J. Zakharov, Nucl. Phys. B136 (1978) 157; M. Glück and E. Reya, Phys. Lett. 83B (1979) 98; J.V. Leveille and T. Weiler, Nucl. Phys. B147 (1979) 147.
- [20] S. Catani, M. Ciafaloni and F. Hautmann, "Production of heavy flavors at high energies" in Physics at HERA, Proceedings of the Workshop, Hamburg, Oct. 29-30, 1991 Eds. W. Buchmüller and G. Ingelman, vol 2, p.690.
- [21] W.H. Press, B.P. Flannery, S.A. Teukolsky, and W.T. Vetterling, Numerical Recipes, Cambridge University Press, 1986, Section 3.6.

### Figure Captions

**Fig.1.**  $h_{A,T,g}^{(1)}(\eta, \xi)$  (eq. (9)) versus  $\eta$  for  $\xi = 10^{-2}$  (solid line),  $\xi = 1$  (dotted line),  $\xi = 3.16$  (short-dashed line),  $\xi = 31.6$  (long-dashed line) and  $\xi = 316$  (dot-dashed line).

**Fig.2.**  $h_{F,T,g}^{(1)}(\eta, \xi)$  (eq. (10)) versus  $\eta$  for  $\xi = 10^{-2}$  (solid line),  $\xi = 1$  (dotted line),  $\xi = 3.16$  (short-dashed line),  $\xi = 31.6$  (long-dashed line) and  $\xi = 316$  (dot-dashed line).





This figure "fig1-1.png" is available in "png" format from:

<http://arxiv.org/ps/hep-ph/9411431v1>

This figure "fig1-2.png" is available in "png" format from:

<http://arxiv.org/ps/hep-ph/9411431v1>